Innovare Academic Sciences

International Journal of Pharmacy and Pharmaceutical Sciences

ISSN- 0975-1491 Vol 7, Issue 11, 2015

Original Article

MONTELUKAST SPRAY DRIED MICROPARTICLES: PREPARATION, EXCIPIENTS SELECTION AND *IN VITRO* PULMONARY DEPOSITION

ROXANE ABDELGAWAD MOUSSA*, RIHAB OSMAN, GEHANE A. S. AWAD, NAHED MORTADA

Department of Pharmaceutics and Industrial Pharmacy, Faculty of Pharmacy, Ain Shams University, Egypt, PO box:1566.
Email: roxaneserageldine@yahoo.com

Received: 24 Aug 2015 Revised and Accepted: 03 Oct 2015

ABSTRACT

Objective: This study focused on the preparation of montelukast sodium (MTK) fast release pulmonary targeted microparticles using the spray drying technique.

Methods: The effect of addition of different excipients namely: mannitol, leucine and ovalbumin on the physico-chemical characteristics of MTK spray dried powders were investigated. Powder flow properties, drug association efficiency as well as microparticle size and mass median aerodynamic diameter (MMAD) were determined. The prepared microparticles were characterized using FT-IR and TGA. The powder crystallographic and thermal properties were studied using DSC and X-ray powder diffraction. A twin stage impinger was used to evaluate *in vitro* pulmonary deposition from which the inhalation indices were derived.

Results: The tested excipients showed no adverse chemical interactions with the drug based on FT-IR. The best inhalation indices were obtained with powders spray dried with leucine followed by leucine/mannitol mixtures with MMAD of 1.73±0.08 and 1.36±0.16 and fine particle fraction of 60.55±1.63 and 52.31±3.52, respectively. The dried powders showed good physico-chemical stability for up to 6 mo storage.

Conclusion: The developed MTK spray dried particles may offer a good platform for the targeted pulmonary delivery of MTK overcoming the major biological barriers.

Keywords: Montelukast, Spray drying, Microparticles, Pulmonary delivery, Mannitol, Albumin, Leucine.

INTRODUCTION

The use of targeted pulmonary delivery systems is an effective means of delivering active drugs to the respiratory system. Presently, there is a particular research interest in pulmonary delivery of drugs, not only for local, but also for systemic effect. This is primarily due to the important advantages offered by the pulmonary route, especially when considering respiratory tract diseases [1, 2].

Montelukast (MTK), see structure shown in fig.1, is a leukotriene-receptor antagonist. This class of medication acts by blocking the effects of the cysteinyl leukotrienes, the main proinflammatory mediators contributing to the pathology of bronchial asthma [3]. Asthma is a complex disorder involving genetic predisposition or environmental factors. It results in severe structural and functional changes in the respiratory zones of the lungs leading to bronchial hyper responsiveness and air flow obstruction thereby causing serious discomfort [4].

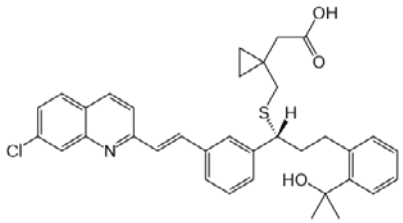

Fig. 1: Montelukast chemical structure

MTK is widely used orally in the management of chronic asthma due to its unique hybrid anti-inflammatory and bronchodilator effects [5]. However, its oral administration has been associated with side effects including headache, drowsiness, gastrointestinal disturbances, sleep disorders, hyper-sensitivity reactions, and increased bleeding tendency with a higher incidence of Churg–Strauss syndrome [6]. Development of targeted pulmonary delivery systems for MTK can increase receptor occupancy, decrease dose, maximize the therapeutic benefits while decreasing the occurrence of systemic side effects [1].

To effectively target the lung, small particles with aerodynamic diameter in the range of 2-5 µm are usually preferred [7]. Particles larger than 5 µm usually impact in the upper respiratory tract, while smaller particles (1-5 µm) deposit by sedimentation under the effect of gravity. Very small particles (<0.5 µm) can diffuse by Brownian motion in the bronchi, terminal bronchioles and alveoli [8]. Meanwhile, in order to achieve rapid infiltration in the airways, deep deposition in alveoli, where thinner alveolar epithelium associated with alveoli large surface area, is favored. This stems from the fact that the epithelial absorption barrier decreases and the absorption increases as a function of the particle penetration depth into the lung. Furthermore, particles depositing in the bronchioles are normally trapped by ciliated cells and moved with the mucus blanket where they are typically exhaled as foreign bodies [9, 10].

In spite of the thin epithelial barrier (0.2 mm) in the alveolar region, the freely roaming macrophages that engulf particles by endocytosis represent a potential obstacle for the fate of the particles. Macrophages can digest them and slowly migrate with their payload up and out of the respiratory tract, either along the mucociliary escalator or entering (to a lesser degree) the lymphatic system [9]. Literature pointed out to several strategies to overcome such barrier: coating of microparticles (MPs) with either the endogenous naturally occurring lung surfactant (dipalmito-phosphatidyl choline) or the hydrophilic polyethylene glycol presented a chemical camouflage to the macrophages [11, 12]. The use of nano-in MPs, large porous particles or rapidly dissolving particles are examples of physical camouflages based on the particle size [13]. Typically, macrophages start engulfing the particles within 5 min reaching maximum after 30 min as reported in earlier studies [14].

To evade the impact of respiratory tract barriers and ensure optimal delivery to the target site, it is imperative to develop appropriate

carriers using biocompatible excipients. Engineering particles with aerodynamic properties fulfilling the above criteria had been lately the theme of many studies where various preparation methods were adopted [13]. Among these methods, the single step spray drying procedure has shown great success. Monitoring the spray drying parameters, namely: feed concentration, pump flow rate, aspiration as well as temperature with careful selection of excipients and carriers are the main controlling factors governing the process yield.

Tailoring the particles aerodynamic properties with mannitol, albumin and leucine were the main focus of this study. Mannitol is a crystalline, stable spray dried matrix former and has recently been approved by regulatory authorities for inhalation use [15, 16]. Sugars are known to act as drying protectants during fast removal of water by spray or freeze drying [17]. Motivated by its proven ability to shape the particles providing respirable powders with high deep lung deposition [18, 19], albumin was also suggested as a particle shaper additive. As a low density surfactant, leucine was used due its previously reported ability to act as a dispersing aid.

Accordingly, the ultimate goal of the present study was to tailor MTK loaded spray dried powders (SDP) for pulmonary administration. The effect of the chosen excipients on the physico-chemical characteristics and flow properties of the SDP were investigated. *In vitro* pulmonary deposition was characterized using a twin stage impinger.

MATERIALS AND METHODS

Materials

Montelukast sodium (MTK): sincerely given by Glaxo Smith-Kline, Egypt. L-Leucine: purchased from Fluka Switzerland. Mannitol: from El Nasr Pharmaceutical Chemicals (ADWIC), Abo Zaabal, Cairo, Egypt. Ovalbumin (grade 2) purchased from Sigma-Aldrich, UK. All other chemicals and reagents were of analytical grade.

Methods

Microparticles (MPs) preparation

The drug and excipients were dissolved, each individually, in water containing 30% ethanol then mixed together. The prepared hydroalcoholic solutions, containing 1% w/v total solids were spray dried with a Buchi B-290 mini spray dryer using the following parameters: inlet temperature: 80 °C, aspiration rate: 85% and pump flow rate: 5%. The resultant outlet temperature was 48±1°C. Table 1 shows the composition of the prepared formulae.

Table 1: Composition of MTK loaded spray dried formulae

Component	Formulae composition % (w/w)				
	D	DM	DL	DA	DML
MTK	100	50	50	50	50
Mannitol	-	50	-	-	25
Leucine	-	-	50	-	25
Ovalbumin	-	-	-	50	-

Powder characterization

Yield determination

The yield values of SDP were determined gravimetrically as percentage of the original amounts of solid contents used [7].

Drug content determination

For drug content determination, expressed as association efficiency (AE) and drug loading capacity, an accurate weight of each SDP formula was dissolved in de ionized water containing 30% v/v of ethanol. The UV absorbances were measured at the predetermined λ_{max} and the drug content in each formula was evaluated from the line equation of a previously constructed calibration curve. MTK association efficiency, theoretical and actual loading were calculated using to equations 1-3.

Powder flow properties

The flow properties of the SDP were evaluated by determining the bulk and tapped densities, Carr's compressibility index (CCI), Hausner's ratio (HR) and the angle of repose (Θ).

For density determination, a certain weight of each SDP was introduced into a small volumetric cylinder, the volume was adjusted by tapping twice and the volume occupied by the powder was noted (bulk volume or Vb). The cylinder was tapped several times (about 100 times) on a solid surface till constant volume and the new volume occupied by the powder was recorded (tapped volume or Vt). The bulk and tapped densities were calculated as shown in equations 4 and 5 [20]. Based on the calculated bulk and tapped densities, Carr's compressibility index (CCI) and Hausner's ratio (HR) were also calculated as shown in equations 6 and 7 [21].

The static angle of repose (Θ) was determined by pouring a certain weight of each SDP through a glass funnel on to a flat collection surface till the required height (1 cm) was achieved and a cone was obtained. The angle to the horizontal surface (angle of repose) was calculated as shown in equation 8 [20, 22].

Particle size measurement and calculation of mass median aerodynamic diameter (MMAD)

The particle size was measured by the wet dispersion method (Laser diffraction-Malvern Mastersizer S, UK) using isopropanol as anti solvent [7]. The size distribution was expressed in terms of D[v,10], D[v,50], D[v,90] and D[4,3] which are the diameters at 10, 50 and 90 percentile cumulative volume and the volume mean diameter, respectively. The span index, defined as the difference between 90 and 10% cumulative volumes, divided by the 50% cumulative volume, was also recorded.

$$\text{MTK association efficiency} = \frac{\text{Actual MTK amount}}{\text{Theoretical MTK amount}} * 100 \quad \text{.....Equation1}$$

$$\text{Theoretical MTK loading capacity} = \frac{\text{Theoretical MTK amount}}{\text{Powder weight}} * 100 \quad \text{..... Equation 2}$$

$$\text{Actual MTK loading capacity} = \frac{\text{Actual MTK amount}}{\text{Powder weight}} * 100 \quad \text{..... Equation 3}$$

$$\text{Bulk density} = \frac{\text{Powder weight}}{\text{Bulk volume}} \quad \text{..... Equation 4}$$

$$\text{Tapped density} = \frac{\text{Powder weight}}{\text{Tapped volume}} \quad \text{..... Equation 5}$$

$$\text{CCI} = \frac{(\text{Tapped density} - \text{Bulk density})}{\text{Tapped density}} * 100 \quad \text{.....Equation 6}$$

$$\text{HR} = \frac{\text{Tapped density}}{\text{Bulk density}} \quad \text{..... Equation 7}$$

$$\tan\theta = \frac{\text{Height (1 cm)}}{\text{Radius of the circle formed at the base of the cone}} \quad \text{..... Equation 8}$$

The mass median aerodynamic diameter (MMAD) was calculated as follow:

$$\text{MMAD} = \text{dg}\sqrt{\frac{\rho}{\rho a}} \quad \text{..... Equation 9}$$

Where ρ is the mass density of the particle (tapped density), ρa is the unit density (1 g/cm^3) and dg is the cumulative geometric volume 50% diameter [10, 23].

Thermogravimetric analysis (TGA)

The residual water content in selected SDP was determined by heating the sample from 30 °C to 150 °C at a rate of 10 °C/min using a thermogravimetric analyzer (Perkin Elmer, Pyris I-Wellesley, USA). The percentage weight change of the sample was measured as its water content was evaporated and was expressed as percent of the initial powder weight.

X-ray powder diffraction (XRPD)

XRPD was used to determine the presence of crystalline and amorphous contents in selected SDP formulations. A Philips PW 3710 XRPD, operated at 45 kV, 30 mA, and scanning angles of 5 ° to 45 °, was used to investigate the powder crystal structure.

Differential scanning calorimetry (DSC)

DSC analysis was performed to study the thermal properties of the pure drug as received and after spray drying with the excipients. For the pure drug, an amount of powder (2-3 mg) was loaded in an aluminum pan under dynamic nitrogen purged at 30 mL/min, then heated from room temperature to 200 °C at 10 °C heating rate, the temperature was held for 15 min after which the sample was cooled to 30 °C at 10 °C/min. The temperature was hold for 1 min, then the sample was reheated to 200 °C at 10 °C/min [7]. DSC was studied on selected formulae using only one heating cycle from room temperature to 200 °C at 10 °C/min heating rate was used.

Fourrier transform infrared spectroscopy (FT-IR)

FT-IR spectra of drug, excipients, 1:1 physical mixtures of MTK with each excipient and selected SDP formulae were recorded using potassium bromide (KBr) disc method. Each sample was gently triturated with powdered KBr in a weight ratio of 1:100 and then pressed using a hydrostatic press at a pressure of 10 tons for 5 min. The disc was placed in the sample holder and was scanned from 4000 to 450 cm^{-1}. All spectra were recorded at ambient temperature under the vacuum to remove air humidity contribution at a resolution of 4 cm^{-1} and 16 times scanning for each measurement to obtain an adequate signal to noise ratio.

***In vitro* pulmonary deposition**

In vitro pulmonary deposition of selected SDP formulae was determined experimentally using a glass twin stage impinger (TSI) as previously reported [24]. Briefly, accurately measured volumes (7 and 30 mL) of collecting solvent (30% ethanol in water) were placed in the upper and lower chambers of the impinger, respectively. Aliquots of SDP (30 mg) were loaded in size No. 3 hard gelatin capsules which were placed each in the dry powder inhaler device (*Aerolizer*®). The capsule was pierced, the inhaler was attached to the throat of the impinger and the powder was drawn through the TSI at an air flow rate of 60 L/min operated for 2x5 seconds aspirations. The capsule was then removed from the device and the empty capsule was weighed to find the remaining non delivered amount of powder [25]. The device (inhaler) was washed and the mouth, throat and device washings were collected in 25 mL volumetric flask. The upper impinger stage (stage 1) washings were collected in a 50 mL volumetric flask while a 100 mL volumetric flask was used for the lower stage (stage 2).

The upper impingement chamber is designed such that at a flow rate of 60 L/min through the impinger, the particle cut-off is 6.4 µm. Particles, smaller than 6.4 µm, pass into the lower impingement chamber and constitute the respirable fraction or fine particle fraction (FPF). The emitted fraction (EF), defined as the percent of total loaded powder mass exiting the capsule [7], was determined gravimetrically as follow:

$$\text{EF} = \frac{(\text{m FULL} - \text{m empty})}{\text{m powder}} * 100 \quad \text{..... Equation 10}$$

Where EF is the emitted fraction, m full and m empty are the masses of the capsules before and after simulating the inhalation respectively and m powder is the mass of the powder.

The fine particle fraction (FPF) was calculated as ratio of FPD to the emitted dose; where fine particle dose (FPD)< 6.4 µm aerodynamic diameter at a flow rate of 60 L/min was defined as the mass of drug deposited in the lower stage of the TSI [26].

$$\text{FPF} = \frac{\text{S2}}{\text{EF}} \quad \text{..... Equation 11}$$

The Effective inhalation index was calculated as follow [27]:

$$\text{EI} = \sqrt{\text{EF} * \text{S2}} \quad \text{..... Equation 12}$$

Where EF is the fraction % emitted from the inhalation system, and S2 is the fraction % distributed to stage 2 of the TSI. The UV absorbance of each collected fraction was measured and the drug present at each stage was calculated from a previously constructed calibration curve.

***In vitro* release study**

An accurately weighed amount of selected SDP corresponding to 2.5 mg drugs was added to 250 mL of 0.03M phosphate buffer solution containing 30% ethanol to allow for sink conditions [28]. The flasks were placed in a shaking water bath at 30 strokes/min at a temperature of 37±0.5 °C. Samples were taken at different time intervals (2, 5 and 15 min), centrifuged and the supernatants were analyzed for their drug content spectrophotometrically using a previously constructed calibration curve in the same medium.

Stability study

Samples of selected SDP formulae were reanalyzed for their total drug content and *in vitro* pulmonary deposition using the TSI after 3 and 6 mo of storage in desiccators at room temperature (25±2 °C) [29].

Statistical analysis

All data are expressed as mean of three determinations±standard deviation (s. d.). The experimental data were analyzed statistically using Graph Pad Prism program by which either the student's t test (when comparing means of two groups) or by analysis of variance (ANOVA, for more than two groups). Differences were considered significant at p≤ 0.05.

RESULTS AND DISCUSSION

Yield, drug association efficiency and loading capacity

Spray drying MTK, without any additives, yielded a powder which tended to agglomerate following spray drying. Clumps were noticed within two days after preparation and storage in desiccators. This could be explained by the effect of fast moisture removal during spray drying resulting in a highly hygroscopic product as noted also in previous studies [30].

Another possible explanation could be the crystallization that might occur during storage of amorphous SDP, causing stickiness and aggregation [31]. Hence, to overcome MTK agglomeration, the use of additives was tried.

Table 2 depicts that 72.4±2.45 % of the drug amount was recovered following spray drying its hydroalcoholic solution free from any other additive. Addition of excipients in a concentration of 50% increased the yield significantly (p≤ 0.05) in case of mannitol, leucine and mannitol/leucine mixture with 83.07±1.33, 90.4±1.65 and 86.70±0.95% respective yield values for formulae DM, DL and DML. Similarly, the effect of leucine and mannitol in improving SDP yields had been reported previously by other investigators [32]. On the contrary, ovalbumin caused a significant decrease (p≤ 0.05) in yield value which reached 50.69%. Sticking of the powder on the cyclone wall noticed during spray drying the drug with ovalbumin accounted for the high loss. Moreover, clumping and agglomeration occurred following co-spray drying the drug with ovalbumin at this concentration (50% w/w).

Table 2: Yield values, drug association efficiency and loading capacity in the spray dried powders formulae

Formula code	Yield values (%)	AE (%)	MTK loading (%w/w)	
			Theoretical	Actual
D	72.40±2.45	-	100	-
DM	83.07±1.33	99.89±2.9	50	49.94±1.45
DL	90.40±1.65	94.75±0.81	50	47.37±0.40
DA	50.69±4.83	96.72±1.15	50	48.36±0.57
DML	86.70±0.95	104.66±1.80	50	52.33±0.90

*Results are mean of three determinations±s. d.-: Not determined.

High association efficiencies, exceeding 90%, were achieved with all formulae. The assayed MTK contents were very close to the theoretical values inferring that only small amounts of drug were lost during the preparation process.

Powder flow properties

As shown in table 3, Formula DM prepared with 50% mannitol, exhibited higher bulk and tapped densities than DL and DML. As expected, higher densities were obtained after tapping and the increase was higher in case of the former formula denoting larger inter particular voids compared to the other 2 formulae.

The decrease in density noted after replacing a part of mannitol with leucine stands behind the preferred use of the later during spray drying of powders intended for pulmonary administration.

As a low density surfactant, it precipitated early on the surface of the evaporating droplet improving the particle de-agglomeration and reducing the bulk density of drug/carrier particles [31].

Table 3: Flow properties of MTK loaded spray dried formulae

Code	Bulk density (g/cm^3)	Tapped density (g/cm^3)	Carr's index (%)	Hausner's ratio	Angle of repose (°)
DM	0.35±0.015	0.59±0.034	40.36±1.30	1.67±0.03	46.55±0.58
DL	0.14±0.002	0.18±0.005	31.95±0.85	1.47±0.01	40.81±0.41
DML	0.24±0.008	0.38±0.014	37.60±0.45	1.60±0.01	43.60±0.68

*Results are mean of three determinations±SD.

The observed CCI, HR and angle of repose ranged from 31.95 to 40.36%, 1.47 to 1.67 and 40.5 to 46.55°, respectively. It is worthy to mention here, that because of the small amounts of powder and the work on the small scale, the differences between the powers could not be clearly seen and almost all formulae showed cohesiveness based on the classification mentioned in literature [33-35].

It should also be pointed out that it was not possible to accurately determine the flow properties of the drug spray dried alone or with ovalbumin due to the previously explained agglomeration yielding false results for flow properties. The best flow properties expressed were achieved with formula DL prepared with 50% leucine.

Particle size and mass median aerodynamic diameter

From table 4, we could observe that 90% of the particles were less than 5 µm indicating suitability for pulmonary administration [36]. Due to the low density of the particles, the theoretical MMAD was found to be lower than their geometric particle size.

Thermogravimetric analysis (TGA)

TGA was performed on representative formulae DM and DL and no residual water was found in both formulae. None of the formulae exceeded 3% of water, the upper limit of moisture characterizing a dry powder as identified in previous studies [37]. Hence, the selected spray drying parameters was suitable to produce dried powders with minimal residual moisture.

X-ray powder diffraction

In accordance with previously reported data, the X-ray diffractogram of pure MTK, fig. 2a, reveals diffused peaks characteristic of its very low crystallinity [38]. On the other hand, the diffractogram of leucine, fig. 2b, shows characteristic peaks at 5°, 25° and 31° indicating high crystallinity. Similarly, the X-ray diffractogram of mannitol, fig. 2c, reveals crystalline peaks at 10.56, 14.71° denoting the presence of beta polymorph. Other lower intensity peaks could also be detected in mannitol diffractogram at 19, 24, 40 and 45°. From fig. 2d we could conclude the presence of albumin in the amorphous form which could be the reason of the agglomeration observed in DA formula.

Table 4: Particle size and MMAD of MTK loaded spray dried formulae

Code	D[4,3] (µm)	Span	Distribution percentile volume (µm)			MMAD (µm)
			10%	50%	90%	
DM	2.26±0.11	1.91±0.08	0.54±0.01	1.98±0.06	4.32±0.28	0.59±0.03
DL	3.17±0.38	1.60±0.31	0.59±0.16	3.22±0.61	5.64±0.18	1.73±0.08
DML	2.53±0.03	2.06±0.03	0.57±0.01	2.16±0.01	5.01±0.09	1.36±0.16

Results are mean of three determinations±SD MMAD: mass median aerodynamic diameter and D [4, 3]: Volume mean diameter.

Spray dried formula DM diffractogram, fig. 2e, shows mannitol characteristic peaks at 19, 24. 40, 45 with lower intensity that the pure excipient. Mixing with the drug followed by spray drying can justify the noted decrease in peaks intensity [39]. The change of the position of some peaks might denote the crystallization of mannitol into another polymorph. This crystallization had already been reported in many references and depended on the spray drying conditions [40].

Similarly, leucine characteristic peaks can still be seen after spray drying with the drug as shown in fig. 2f. Previous studies postulated that above a threshold level, 10% leucine concentration in that work, leucine crystallinity peaks were still seen after spray drying [41]. We can thus conclude that the produced spray dried powders (formulae DM and DL) were crystalline in nature probably due to the presence of leucine and mannitol at 50% concentration.

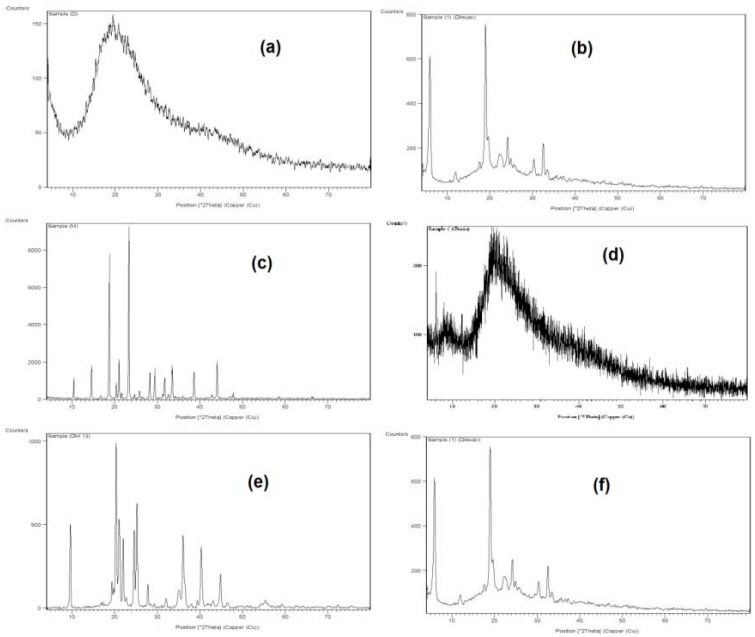

Fig. 2: X-ray diffractograms of pure (a) drug, (b) leucine, (c) mannitol, (d) albumin and formulae (e) DM and (f) DL

Differential scanning calorimetry (DSC)

In order to study the thermal properties of the drug, it deemed necessary to use two heating cycles. The first one was used to get rid of the drug associated water as the result of its highly hygroscopic nature [42, 43]. In the second heating cycle, in fig. 3, the broad water endotherm, seen before 100°C, disappeared due to the volatilization of water and only one small broad endotherm was seen at 149°C. This peak corresponded to the drug melting previously mentioned in literature[44].

As shown in fig. 4, mannitol exhibits a single sharp endothermic peak at about 171°C corresponding to its melting point [45]. This peak can also be seen in DM containing 50 % of mannitol but with a much lower intensity. Furthermore, in spite of the spray drying process, the obtained powder (DM) showed some crystallinity attributed to the presence of mannitol at this high concentration (50%) confirming the results obtained from XRPD. Leucine melting endotherm was not shown in its thermogram as it normally melts at 296 °C, higher than the used temperature range in this study [46]. A similar observation could also be seen in case of DL.

Fourrier transform infrared spectroscopy (FT-IR)

To investigate the interaction between the components of SDP, FT-IR studies were conducted. MTK pure drug, fig. 5, shows the bond vibrations at 3355 cm^{-1} (COOH stretching), 3058.3 cm^{-1} (aromatic CH stretching), 2974.3 cm^{-1} (aliphatic CH stretching) [47]. Other peaks observed at 1636.3 cm^{-1} corresponded to C=O stretching, at 1562.6 and 1595 cm^{-1} are the C-C aromatic stretch, while at 1495 cm^{-1} appeared the C-C alkane stretch, 1136 cm^{-1} C-O stretch of alcohol, 960 cm^{-1} OH bend and 697.8 cm^{-1} sharp peak corresponded to =C-H bend of alkenes.

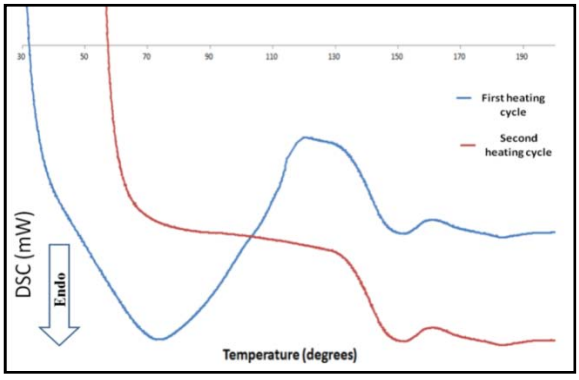

Fig. 3: DSC thermogram of MTK as received

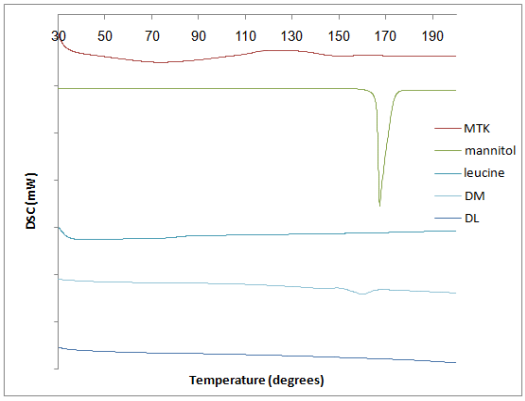

Fig. 4: DSC thermograms of MTK, excipients, MTK/physical mixtures and selected spray dried formulae

Mannitol FT-IR spectrum, fig. 5, shows the free alcoholic OH stretch between 3200-3500 cm^{-1}, CH stretch of alkane peaks between 2906-2970 cm^{-1} could also be depicted. A medium peak at 1459 cm^{-1} attributed to CH bending, two sharp peaks at 1019 cm^{-1} and 1082 cm^{-1} corresponding to C-O alcoholic stretch could also be seen in the spectrum.

Leucine FT-IR spectrum shows characteristic peaks at 3402 and 3056 cm^{-1} corresponding to the asymmetric valence vibrations of the ammonium group and the free carboxylic OH broad peak respectively. CH alkane stretch could be seen at 2959 and 2871 cm^{-1}, while the characteristic peak at 2129 cm^{-1} corresponded to symmetric valence vibration of the ammonium group.

It could be seen that the spectrum of MTK/mannitol physical mixture is a simple superposition of the spectra of both components. In the spray dried formula DM, mannitol peaks are more prominent and of higher intensity than in the physical mixture. For leucine containing formulae (physical mixture or spray dried), it is obvious that the drug peaks were completely masked or merged with leucine bands. To sum up, no disappearance nor major shift was noted in the characteristic bands of MTK when combined with the selected excipients in the spray dried formulae. Hence, no obvious incompatibilities could be detected with the chosen additives.

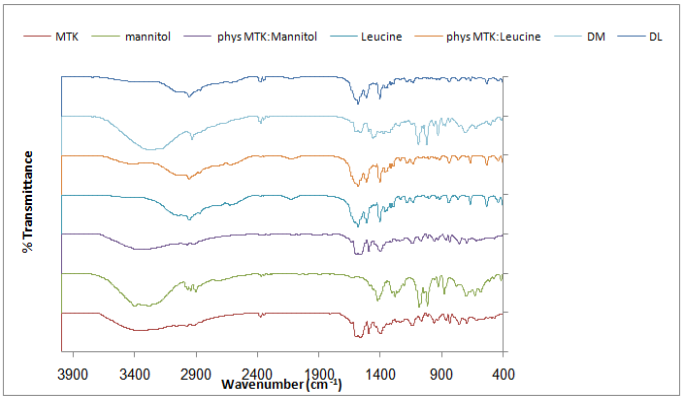

Fig. 5: FT-IR spectra of MTK, excipients, their physical mixtures and selected spray dried formulae

In vitro pulmonary deposition

The effect of the formulation variables on the *in vitro* pulmonary deposition was studied using TSI. The drug percent deposited in mouth/throat and device (D/M/T) and in stages 1 and 2 are illustrated in fig. 6. The inhalation indices namely ED, FPF and EI were calculated and are presented in table 5.

Early deposition of a large fraction from formula DM was seen in D/M/T and in stage 1 probably due to its previously demonstrated poor flow characteristics. On the other hand, very fluffy fine light particles of formula DL gave this formula the chance of travelling deeper in the device, thus deposited in stage 2. Replacing a part of mannitol with leucine greatly improved the stage 2 deposition as well as all inhalation indices as shown in DML compared to DM.

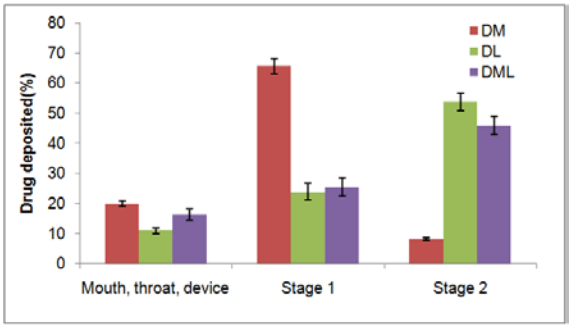

Fig. 6: *In-vitro* pulmonary deposition of MTK spray dried formulae using TSI

Table 5: Inhalation indices of MTK spray dried formulae

Code	Inhalation indices %		
	ED%	FPF%	EI%
DM	93.87±3.08	8.87±0.37	27.96±0.52
DL	88.69±1.95	60.55±1.63	69.02±1.66
DML	87.78±5.75	52.31±3.52	63.47±3.76

*Results are mean of three determinations±s. d., ED: emitted dose, FPF: fine particle fraction, EI: effective inhalation index.

In vitro release study

Fig. 7 shows that MTK dissolved at a faster rate following its spray drying releasing 95 % of the drug in 5 min. Similarly, an instantaneous release of MTK was seen with the SDP formulae DM, DL & DML where 100% release was achieved in less than 15 min. This fast release is of special importance when considering pulmonary delivery. This does not only provide fast drug onset of action but also can guarantee avoidance of uptake and engulfment by the rooming alveolar macrophages.

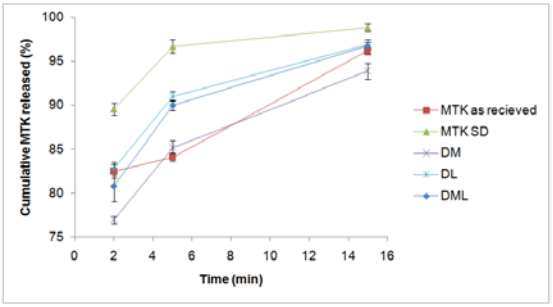

Fig. 7: *In vitro* release study of MTK SD formulae in 0.03M phosphate buffer solution containing 30% ethanol at 37 ℃ and 30 stroke/min (mean±SD, n = 30). *For formulae composition, refer to table 1

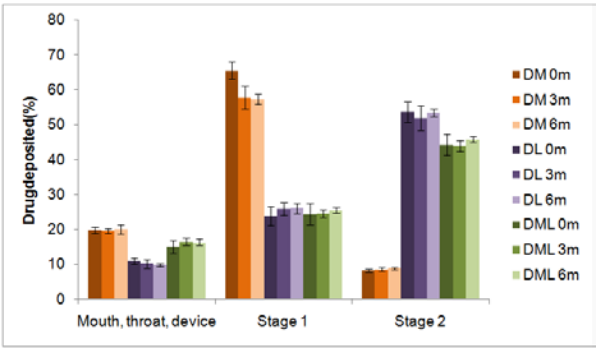

Fig. 8: *In vitro* pulmonary deposition of MTK loaded SDP determined using TSI.

Table 6: MTK association efficiency after storage at various times intervals

Formula	Association efficiency (%) at various time intervals		
	Fresh	3 Mo	6 Mo
DM	96.76±0.77	96.24±1.18	95.63±0.66
DL	94.75±0.81	94.94±0.92	94.86±0.51
DML	96.54±2.90	96.76±0.76	96.58±0.42

*Results are mean of three determinations±SD No statistically significant changes in drug association efficiency (table 6) or deposition in TSI (fig. 8) with storage could be detected with the selected formulae indicating their stability.

Stability study

To evaluate the long term stability, the total drug content and the *in vitro* pulmonary deposition for selected formulae, DM, DL and DML), were evaluated after storage for three and six months. As shown in table 6, the data were compared to those obtained with the freshly prepared formulae.

CONCLUSION

The ultimate goal of the study was to prepare stable targeted pulmonary delivery system of MTK using the spray drying technique. To improve the stability of MTK following spray drying, hydro alcoholic mixtures of MTK and different excipients were spray dried. Ovalbumin produced sticky unstable powders with very low yields. Mannitol was found to produce dense particles with small particle size, poor flow properties and low respirable fraction. Leucine significantly improved flow properties, providing powders with high inhalation indices. DSC and X-ray studies revealed the crystallinity of the spray dried powders which probably contributed to the enhanced stability and flow characteristics of the powders. The fast release of the drug and immediate dissolution of the powders will be important in avoiding uptake by the highly active alveolar macrophages.

CONFLICT OF INTERESTS

Declared None

REFERENCES

1. Daniher D, Zhu J. Dry powder platform for pulmonary drug delivery. Particuology 2008;6:225-38.
2. Beck-Broichsitter M, Merkel O, Kissel T. Controlled pulmonary drug and gene delivery using polymeric nano-carriers. J Controlled Release 2012;161:214-24.
3. Al-Hamdani F. Comparative clinical evaluation of ketotifen and montelukast sodium in asthmatic Iraqi patients. Saudi Pharm J 2010;18:245-9.
4. Blume C, Davies D. *In vitro* and *ex vivo* models of human asthma. Eur J Pharm Biopharm 2013;84:394-400.
5. Rubinstein I, Kumar B, Schriever C. Long-term montelukast therapy in moderate to severe COPD—a preliminary observation. Respir Med 2004;98:134-8.
6. Lipworth B. Leukotriene-receptor antagonists. Lancet 1999;353:57-62.
7. Osman R, Kan P, Awad G, Mortada N, El-shamy A, Alpar O. Spray dried inhalable ciprofloxacin powder with improved aerosolisation and antimicrobial activity. Int J Pharm 2013;449:44-58.
8. Yang W, Peters J, Williams R. Inhaled nanoparticles-a current review. Int J Pharm 2008;356:239-47.
9. Mobley C, Hochhaus G. Methods used to assess pulmonary deposition and absorption of drugs. Drug Discovery Today 2001;6:367-75.
10. Sung J, Pulliam B, Edwards D. Nanoparticles for drug delivery to the lungs. Trends Biotechnol Sci 2007;25:563-70.
11. Evora C, Soriano I, Rogers R, Shakesheff K, Hanes J, Langer R. Relating the phagocytosis of microparticles by alveolar macrophages to surface chemistry: the effect of 1,2-dipalmitoylphosphatidylcholine. J Controlled Release 1998;51:143-52.
12. Weingart J, Vabbilisetty P, Sun X. Membrane mimetic surface functionalization of nanoparticles: Methods and applications. Adv Colloid Interface Sci 2013;197–198:68-84.
13. Roa W, Azarmi S, Al-hallak M, Finlay W, Magliocco A, Lobenberg R. Inhalable nanoparticles, a non-invasive approach to treat lung cancer in a mouse model. J Controlled Release 2011;150:49-55.
14. El-Sherbiny M, El-Baz M, Yacoub M. Inhaled nano-and microparticles for drug delivery. Global Cardiol Sci Practice J 2015;2:1:14.
15. Daviskas E, Anderson S, Eberl S, Young I. Beneficial effect of inhaled mannitol and cough in asthmatics with mucociliary dysfunction. Respir Med 2010;104:1645-53.
16. Yamasaki K, Kwok P, Fukushige K, Prud'homme R, Chan H. Enhanced dissolution of inhalable cyclosporine nano-matrix particles with mannitol as matrix former. Int J Pharm 2011;420:34-42.
17. Wu L, Miao X, Shan Z, Huang Y, Li L, Pan X, *et al.* Studies on the spray dried lactose as carrier for dry powder inhalation. Asian J Pharm Sci 2014;9:336-41.
18. Zeng X, Martin G, Marriott C. Preparation and *in vitro* evaluation of tetrandrine-entrapped albumin microspheres as an inhaled drug delivery system. Eur J Pharm Sci 1995;3:87-93.
19. Chan H. Dry powder aerosol drug delivery-opportunities for colloid and surface scientists. Colloids Surf A 2006;284–285:50-5.
20. Puttewar T, Kshirsagar M, Chandewar A, Chikhale R. Formulation and evaluation of orodispersible tablet of taste

masked doxylamine succinate using ion exchange resin. J King Saud Univ Sci 2010;22:229-40.
21. Traina K, Cloots R, Bontempi S, Lumay G, Vacewalle N, Boschini F. Flow abilities of powders and granular materials evidenced from dynamical tap density measurement. Powder Technol 2013;235:842-52.
22. Awasthi R, Kulkarni G. Development and characterization of amoxicillin loaded floating microballoons for the treatment of Helicobacter pylori induced gastric ulcer. Asian J Pharm Sci 2013;8:174-80.
23. Oskouie A, Noll K, Wang H. Minimizing the effect of density in determination of particle aerodynamic diameter using a time of flight instrument. J Aerosol Sci 2003;34:501-6.
24. Geuns E, Toren J, Barends D, Bult A. Decrease of the stage-2 deposition in the twin impinger during storage of beclomethasone dipropionate dry powder inhalers in controlled and uncontrolled humidities. Eur J Pharm Biopharm 1997;44:187-94.
25. Young P, Price R. The influence of humidity on the aerosolisation of micronised and SEDS produced salbutamol sulphate. Eur J Pharm Sci 2004;22:235-40.
26. Le V, Hoang Thi T, Robins E, Flament M. Dry powder inhalers: study of the parameters influencing adhesion and dispersion of fluticasone propionate. AAPS Pharm Sci Tech 2012;13:477-84.
27. Nakate T, Yoshida H, Ohike A, Tokunaga Y, Ibuki R, Kawashima Y. Formulation development of inhalation powders for FK888 using the E-haler® to improve the inhalation performance at a high dose, and its absorption in healthy volunteers. Eur J Pharm Biopharm 2005;59:25-33.
28. Yan C, Wu Q, Zhang Z, Yuan L, Liu X, Zhou L. Preparation of curcumin-loaded liposomes and evaluation of their skin permeation and pharmacodynamics. Molecules 2012;17:5972-87.
29. Zhao Q, Wang T, Wang J, Zheng L, Jiang T, Cheng G, *et al.* Template-directed hydrothermal synthesis of hydroxyapatite as a drug delivery system for the poorly water-soluble drug carvedilol. Appl Surf Sci 2011;257:10126-33.
30. Moreira G, Maia M, Souza A, Brito E, Medeiros M, Azeredo H. Physical properties of spray dried acerola pomace extract as affected by temperature and drying aids. LWT-Food Sci Technol 2009;42:641-5.
31. Ruohui L, Wenjie L, Meng W, Cordelia S, Xiao C. Formation of crystalline amino acid particles via spray drying. Chemeca 2013: Challenging Tomorrow conference; 2013. p. 575-80.
32. Sinsuebpol C, Chatchawalsaisin J, Kulvanich P. Preparation and *in vivo* absorption evaluation of spray dried powders containing salmon calcitonin loaded chitosan nanoparticles for pulmonary delivery. Drug Des Dev Ther 2013;7:861-73.
33. Geldart D, Abdullah E, Hassanpour A, Nwoke L, Wouters I. Characterization of powder flowability using measurement of angle of repose. China Particuol 2006;4:104-7.
34. Shah R, Tawakkul M, Khan M. Comparative evaluation of flow for pharmaceutical powders and granules. AAPS Pharm Sci Tech 2008;9:250-8.
35. Lebrun P, Krier F, Mantanus J, Grohganz H, Yang M, Rozet E, *et al.* Design space approach in the optimization of the spray-drying process. Eur J Pharm Biopharm 2012;80:226-34.
36. Fernández Tena A, Casan Clarà P. Deposition of inhaled particles in the lungs. Archivos de Bronconeumología 2012;48:240-6.
37. Hastedt J, Cabot K, Gong D, Hester D. Storage stable powder compositions of interleukin-4 receptor; 2007.
38. Patil-Gadhe A, Pokharkar V. Montelukast-loaded nanostructured lipid carriers: part I oral bioavailability improvement. Eur J Pharm Biopharm 2014;88:160-8.
39. Sahoo N, Kakran M, Abbas A, Judeh Z, Li L. Preparation, characterization and dissolution behavior of artemisinin microparticles. Adv Powder Technol 2011;22:458-63.
40. Maas S, Schaldach G, Littringer E, Mescher A, Griesser U, Braun D, *et al.* The impact of spray drying outlet temperature on the particle morphology of mannitol. Powder Technol 2011;213:27-35.
41. Feng A, Gwin M, Finlay P, Bennett M, Boraey M, Kuehl P, *et al.* Rational design of microparticels for respiratory drug delivery using L-Leucine. Int J Pharm 2011;409:156-63.
42. Alnabari M, Sery Y, Adin I, Arad O, Kaspi J. Stable amorphous forms of montelukast sodium; 2009.
43. Bilgic M. Stable pharmaceutical combinations; 2010.
44. Mahajan H, Gundare S. Preparation, characterization and pulmonary pharmacokinetics of xyloglucan microspheres as dry powder inhalation. Carbohydr Polym 2014;102:529-36.
45. Hulse W, Forbes R, Bonner M, Getrost M. The characterization and comparison of spray-dried mannitol samples. Drug Dev Ind Pharm 2009;35:712-8.
46. Adhikari S, Kar T. Bulk single crystal growth and characterization of l-leucine–A nonlinear optical material. Mater Chem Phys 2012;133:1055-9.
47. Priyanka K, Abdul Hasan S. Preparation and evaluation of montelukast sodium loaded solid lipid nanoparticles. J. Young Pharm 2012;4:129-37.